4open 2023, **6**, 6

https://doi.org/10.1051/fopen/2023005

Special issue on GDR Cosm'actifs
Guest Editor: Richard Daniellou

Available online at:
www.4open-sciences.org

RESEARCH ARTICLE OPEN ACCESS

Investigation of the link between the human skin relief and the dermal fibers network by coupling topographic analysis and LC-OCT imaging before and during folding tests

Meriem Ayadh[1,2,*], Amaury Guillermin[1], Marie-Angèle Abellan[1], Sara Figueiredo[2], Mélanie Pedrazzani[3], Emmanuel Cohen[3], Armelle Bigouret[2], and Hassan Zahouani[1]

[1] Univ Lyon, Ecole Centrale de Lyon, CNRS, ENTPE, LTDS, UMR5513, 69130 Ecully, France
[2] Laboratoires Clarins, 5 Rue Ampère, 95300 Pontoise, France
[3] Damae Medical, 14 Rue Sthrau, 75013 Paris, France

Received 22 June 2022, Accepted 4 May 2023

Abstract – Knowing the evolution of the skin's response to mechanical solicitations and understanding its origin is important in medicine, surgery, and cosmetics. Studies performed in vitro and ex vivo show that links exist between the topographic skin properties and the collagen and elastin fibers network in the dermis. But, to our knowledge, no in vivo study shows this link. In this study we propose a combination of experimental tests to demonstrate the link between the topographic skin properties and the fibers network in the dermis in vivo. The first method consists in analyzing the skin relief images. The second method uses a recently developed imaging technique of human skin in vivo with a high spatial resolution: Line-field Confocal Optical Coherence Tomography (LC-OCT). This technology provides two types of images modalities: vertical and horizontal section images. The skin relief images and its internal layers are carried out for the skin at rest and during a folding test. The latter is performed using a folding system developed in this study. From these images, we calculate the density of the skin lines printed on the skin surface and their orientations. Thanks to the two modalities of LC-OCT, we obtain the full 3D image of the skin volume. From these images we extract the fibers density and their orientation in the plans parallel and perpendicular to the outer skin surface. The study is carried out on 42 volunteers aged from 20 to 55 years-old. Skin relief analysis and LC-OCT images are performed on the skin of the forearm and thigh. The results show similar distributions of the skin lines on the surface and of its fibers in the volume. We could observe a correlation between the skin lines at the surface and the structure in depth of its layers in the volume ($0.40 < r_{\text{Spearman}} < 0.73$).

Keywords: In vivo test, Skin topography, Skin folding test, LC-OCT imaging

Introduction

Human skin is characterized by the relief of its surface and its complex structure in the volume. This relief is very particular, it depending mainly on the body area, and changes with age [1]. The skin surface is formed by a network of furrows (lines), follicular orifices and sweat pores. It can reflect the state of the underlying skin layers and their biomechanical properties [1]. More specifically the state of the skin surface may reflect the particular state of the dermal layer, which is characterized by its fibers network.

The cutaneous relief can provide information on skin anatomy, functionality and properties [1]. The study and characterization of the skin topography can be a means of evaluating the aging effect, or the application of a medical or cosmetic product [2]. Methods for characterizing the skin relief have been developed to reconstruct the skin surface image in three dimensions. The relief is then analyzed by tactile scanning microscopy (mechanical scanning roughness meter) or optical scanning microscopy (optical roughness meter or defocusing laser microscope) techniques [1]. These techniques consist in scanning the surface under study line by line along an axis perpendicular to the surface. From the image, it is possible to determine parameters characterizing the skin relief such as: the furrows depth, the skin plateaus area, the density and orientation of the furrows, etc. [2].

Guinot et al. [3] were interested in studying skin microrelief to identify skin morphological indicators and their variation with age. These indicators are parameters of skin plateau depth and valleys, plateau area, width and depth of furrows, and density of skin lines as a function of their depth. These parameters allow us to study the

*Corresponding author: ayadhmeriem@gmail.com

evolution of skin relief with age but do not provide any information on skin tension. Zahouani et al. [2, 4] have developed a method for analyzing skin microrelief that allows to study the anisotropy of skin tissue and its evolution with age, as well as to have information on the natural skin tension [5]. This method is based on the calculation of the skin lines density according to their orientation and depth. These lines are oriented in different directions and their orientation depends on the body area. Although the skin lines are oriented in different directions, it has been noticed that they have preferential directions and that they form two families of lines perpendicular to each other [6]. The first family of lines is the family of lines parallel to the Langer lines, and the second family is the family of lines perpendicular to the Langer lines.

In vitro and ex vivo studies [7, 8] show that the cutaneous relief can express the state of the anisotropy of the natural skin tension, and the effect of the various modifications that the skin may undergo over the course of life. However, to the author's knowledge, there is a lack of studies showing if such a link exists in vivo and if a parameter could allow to quantify it.

It is known that each skin layer has different components and therefore specific optical properties [1]. These properties make it possible to distinguish the various components of the skin using imaging techniques. They also give access to the composition of the tissue and its biochemical properties [9, 10]. Several techniques for skin characterization by imaging have been developed. In dermatology and cosmetology, the interest of in vivo skin imaging is obvious. It provides an in-depth view of the skin and of the evolution of the tissues. It gives a patient-designed information of a person after application of a product, lotion or cream. Imaging techniques are non-invasive. This property is very important in case of sensitive or damaged skins. The two important parameters of these techniques are resolution and penetration depth. The thickness of the skin varies from 0.5 to 5 mm depending on its location in the body [1] with very small distance (cellular scale) existing between two components. If the resolution is not sufficient, the information is inaccessible. The resolution limit in some techniques is the reason why it is impossible to have information on a fiber. For example, these techniques include magnetic resonance imaging (MRI) [11], ultrasound [1], optical coherence tomography (OCT) [12], and confocal microscopy [13].

In this study we propose a combination of in vivo experimental tests to show the link between the topographical properties of the skin the surface and the fibers network in the skin volume and more precisely in the dermis. The first method consists in analyzing the images of skin relief of skin at rest and during a folding test. From these images we calculate the density of the skin lines and their orientations. The second method is based on a recently developed imaging technique which allows us to obtain images of the human skin in vivo with very high spatial resolution: Linefield Confocal Optical Coherence Tomography (LC-OCT). To evaluate the links between the data generated by the two approaches, a correlation test is carried out using the Spearman correlation test.

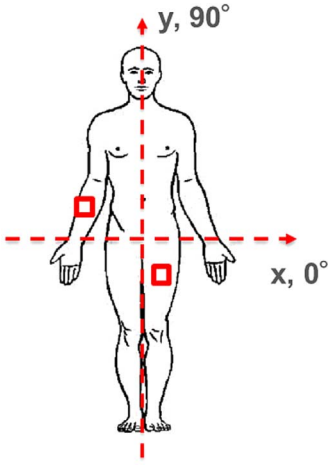

Figure 1. Test zones and body axes.

Material and methods

Panel and test zones

The tests were performed on the right forearm (12 cm above the wrist) and left thigh (12 cm above the knee) (Fig. 1) of 42 French Caucasian women volunteers divided into two groups: a young group [20–30] years old (21 volunteers) and a middle-aged group [45–55] years old (21 volunteers) [14]. All the volunteers participated after giving their informed consent and all the procedures were compliant with the latest revision of the Declaration of Helsinki. The volunteers were non-smokers, in good health and had healthy skin on the forearm and thigh without scars or tattoos. To ensure the homogeneity of the measurements, the volunteers had a Body Mass Index (BMI) between 18.5 and 27 kg/m, a cellulite index less than 2 for the thigh, a phototype between I and III, and all volunteers of the middle-aged group were menopausal. The volunteers did not apply any cosmetic products on the body on the test day. After an acclimatization period of at least 10 minutes the tests were carried out in an air-conditioned room ($T = 21 \pm 2$ °C and $H = 50 \pm 10\%$). The volunteer sits in an armchair (dentist type), legs extended, uncrossed, and slightly bent, right arm resting on an armrest, the palm of her hand up. The volunteer was asked not to move for the duration of the measurements to ensure their homogeneity and to prevent as much noise as possible in the recorded data.

Skin folding test

The study of the skin folding is performed using a skin folding device developed at the Laboratory of Tribology and Dynamic of Systems (Fig. 2) by Guillermin [15]. This device is inspired by the manual diagnostic instrument called DensiScore© [16]. It makes it possible to mimic the action of clinicians by automating and controlling the speed and rate of skin deformation. It is manufactured by 3D printing in acrylonitrile butadiene styrene (ABS) using the Zortrac M200© printer. The deformation and displacement speed are controlled by an automated micrometric

Figure 2. Installation of the skin folding device.

table (PI Stage M663.465, Physik Instrumente©). The moving speed of this table is 180 mm/s, the stroke distance is 20 mm, its size is 33 mm, and its mass is 50 g. The dimensions of this device are: 55 × 35 mm and its total weight is less than 100 g. The system is controlled and operated under LabView© (version 17.0, National Instruments Software, France). The device is bonded to the skin using a hypoallergenic double-sided adhesive (Monaderm – G0203 M). This device therefore allows folds to appear on the skin surface. Skin folding is carried out along the y-axis of the body (Fig. 1) regardless of the body area, with a speed of 10 mm/s and a deformation rate of 32%.

Skin relief

Skin replicas were produced using SILFLO silicone (MONADERM, Monaco) [5]. The replicas are made on the skin at rest (Fig. 3a) and during folding test (Fig. 3b). During the folding test, the SILFLO mixture is spread across the middle of the device to make the imprint of the wrinkled skin. The three-dimensional skin relief was then reconstructed using the chromatic confocal microscopy system (from AltiMet – AltiSurf 500®, France). The images obtained are studied with a program developed by Zahouani [4]. This approach makes it possible to identify the network of skin lines and to extract their density in different directions from 0° to 180° (Fig. 1) with a step size of 20° [5].

Line-field Confocal Optical Coherence Tomography imaging and Folding test (LC-OCT)

The study of the skin structure was carried out by LC-OCT imaging. It is a recently developed imaging technique that allows to image the human skin in vivo with a very high resolution [17–19]. LC-OCT combines two imaging techniques: vertical section (B-scan) and horizontal section (C-scan) images (Fig. 5a). C-scan imaging is obtained using a mirror galvanometer for side scanning with a piezoelectric chip for modulation of the interferometric signal. An almost identical spatial resolution of ∼ 2 µm is measured for B-scans and C-scans. Images are acquired in both modes at a rate of about 10 images per second using a broadband laser with a central wavelength of 1300 nm. The horizontal field of view of C-scans is 1.2 × 0.9 mm, and the vertical field of view of B-scans is 1.2 × 0.4 mm. In vivo cell-scale resolution of human skin is possible in both B-scan and C-scan modes. This technique also allows real-time navigation into the skin tissues, as well as the reconstruction of a stack of three-dimensional images of the tissue volume.

LC-OCT image acquisition was performed on the right forearm and left thigh. Images were taken on the skin at rest (Figs. 4a and 4c) and during the folding tests by coupling the LC-OCT technique to the skin folding device (Figs. 4b and 4d).

The fiber orientations were calculated over the entire 60 µm under the dermo-epidermal junction (DEJ). Orientations were obtained from the skeletonization of the collagen and elastin network using the angular system of spherical coordinates (Fig. 5b). An example of the skeleton of the fiber network in the horizontal plane for the forearm is shown in Figure 5c. The density of the fibers by interval of directions going from 0° to 180° with a step of 20° is extracted in the horizontal and vertical planes.

Statistical analysis

Statistical analysis is performed using the XLStat software (version 2019.4.2, Addinsoft, France). In this study, the non-parametric Mann-Whitney test is performed with a significance level of 5% to assess the significance of the differences observed between the two age groups (young and middle-aged) and the two states of the skin (at rest and during the folding test). To assess the relationship between the data, a correlation test is carried out using the Spearman correlation test. This test provides a correlation coefficient (r) which is the Spearman coefficient. It lies between −1 and 1: if $0.3 < r < 0.5$ (or $-0.5 < r < -0.3$) then the relationship is weak, if $0.5 < r < 0.8$ (or $-0.8 < r < -0.5$) then the relationship is of medium intensity, and if $r > 0.8$ (or $r < -0.8$) then the relation is strong. In this study, only coefficients with a significant associated p-value (<5%) are interpreted. It should be noted that for skin at rest, data from all volunteers are included in correlation test. Contrary for skin during the folding test, correlation tests are carried out only for 5 young volunteers and 3 middle-aged volunteers because only their 3D stacks of folded skin were suitable for this analysis with not too much noise as will be explained in the result section. Only the data of these 8 volunteers (line densities and fiber densities) are used in the correlation test of the folded skin.

Results

Analysis of skin relief

The resulting skin relief images (Table 1) show the difference in the lines pattern printed on the skin surface between the skin at rest and during folding test whatever the body area (forearm and thigh) and whatever the age group (young and middle-aged groups). The densities of these lines extracted from these images allows a quantitative analysis of what is occurring. Table 2 presents the results as a distribution of skin lines according to the directions (from 0° to 180°). These results show, for both body

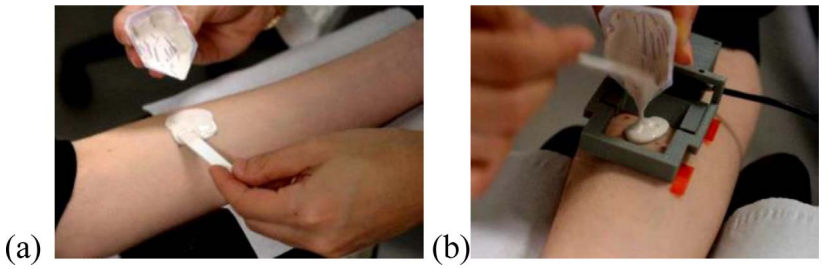

Figure 3. (a) Replica of the skin at rest. (b) Replica of skin during folding test.

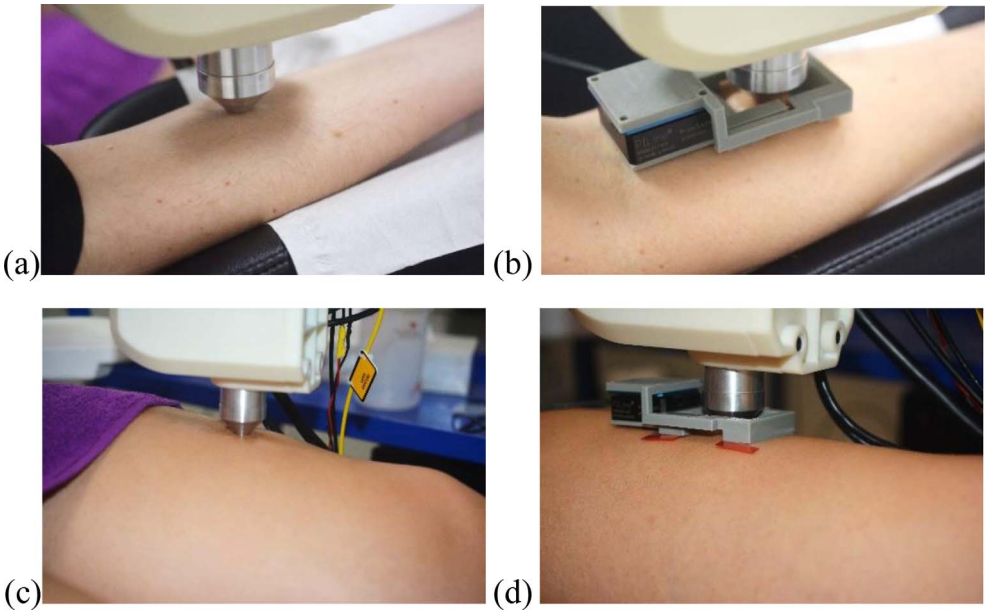

Figure 4. Acquisition of images by LC-OCT of the skin on (a) the forearm at rest, (b) the forearm during folding test, (c) the thigh at rest and (d) the thigh during folding test.

areas and both age groups, that the distribution of skin lines is significantly different (p-value < 0.05) between the skin at rest and during folding test. Skin folding accentuates the orientation of the lines towards directions which depend on the body area: [0° – 40°] and [140° – 180°] for the forearm with a maximum in the preferred directions [40° – 60°] ($d_{\text{young}} = 17.31 \pm 1.70\%$, $d_{\text{middle-aged}} = 15.83 \pm 1.99\%$) and [0° – 20°] for the thigh ($d_{\text{young}} = 22.49 \pm 4.48\%$, $d_{\text{middle-aged}} = 22.36 \pm 4.58\%$).

We also notice an age effect on the images and on the distribution of the lines (Tables 1 and 2). For the young skin at rest, we have a dense network of lines. During folding test for the young skin, the folds move closer together and are not too deep. For older skin at rest, the distance between lines appears to be larger revealing sagging skin, and the folds are deeper during the folding test. It should also be noted that the effect of age is not the same in all directions. For the forearm, the density of the lines increases significantly with age (p-value = 0.004) in the [0° – 20°] directions and decreases (p-value = 0.011) in the [40° – 60°] directions. For the thigh, the density of the lines decreases significantly with age (p-value = 0.040) in the [60° – 100°] directions.

LC-OCT images

Table 1 shows the LC-OCT images of the skin of the forearm and thigh at rest and during the folding test for a young and a middle-aged volunteer as an example. From these images, we extracted the density of skin fibers as a function of direction. Table 2 presents the results as a distribution of skin fibers densities according to direction in the horizontal (azimuthal) and vertical (polar) planes for the forearm and thigh at rest and during folding test for the young and middle-aged groups.

3D image stacks of folding skin are more difficult to study, as the folds created disrupt the organization of the skin layers, making segmentation difficult. For this reason, the extraction of the skin fibers density for the folded skin in the horizontal plane was carried out on the images of 5 young volunteers and 3 middle-aged volunteers which were suitable for this analysis. This partial data analysis was only carried out for the 3D stacks of folded skin. It gives some important information on what occurs during the folding test.

Images in the horizontal plane (Table 1) show the state of the fibers network for the skin at rest and during

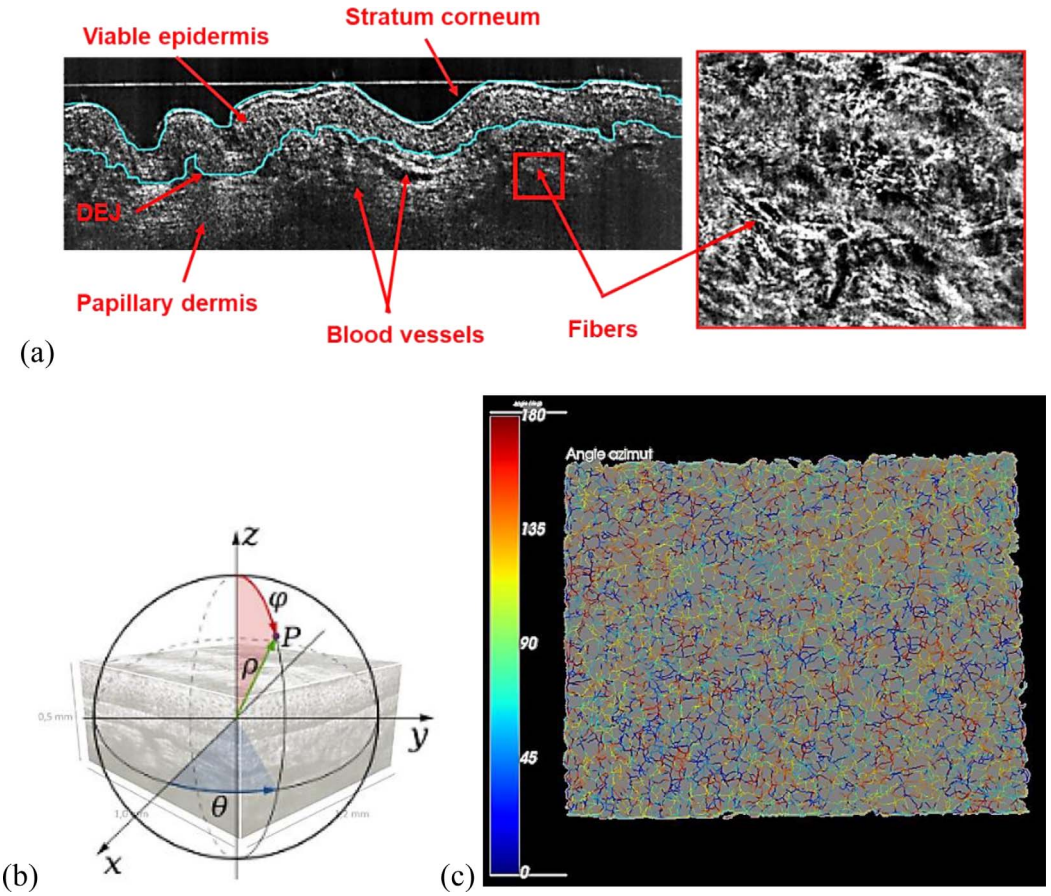

Figure 5. (a) Segmentation of skin layers and DEJ. (b) Identification and definition of angles on a 3D stack. (c) Example of the fibers network skeleton in the horizontal plane for the forearm for a young volunteer.

the folding test for both body areas. As previously mentioned, the folding of the skin disrupts the organization of this fibers network. Consequently, a reorientation of the fibers towards preferential directions can be observed. For the skin at rest, the densities of skin fibers extracted from these images (Table 2) show that for the forearm, the fiber density is maximum in the [40° – 60°] directions for both age groups (d_{young} = 15.76 ± 1.85%, $d_{middle\text{-}aged}$ = 15.50 ± 2.50%). For the thigh, the fiber density is highest in the [20° – 80°] directions for both age groups (d_{young} = 15.57 ± 1.82%, $d_{middle\text{-}aged}$ = 16.06 ± 2.65%). During the folding test, there is a significant reorientation of the fibers towards the [80° – 140°] directions with a maximum in the
[40° – 80°] directions for the forearm (d_{young} = 15.28 ± 1.20%, $d_{middle\text{-}aged}$ = 13.54 ± 0.10%) and [80° – 100°] for the thigh (d_{young} = 16.17 ± 2.10%, $d_{middle\text{-}aged}$ = 13.77 ± 1.50%).

LC-OCT images in the vertical section depict the state of the skin layers at rest and the effect of folding on these different skin layers. All skin layers respond to the applied solicitation, whether in young or middle-aged volunteers. For the skin at rest, the fiber density is highest in the [60° – 120°] directions for the forearm and thigh. During the folding test, no significant difference is observed. The fibers remain oriented in these directions. The orientation of fibers in these directions which are almost perpendicular to the skin surface leads to the following question: Do the fibers oriented in these directions correspond to elastin fibers? The answer to this question is not yet available. Information on the diameters of the fibers according to their direction could help to find an answer.

The results of the distribution of fibers in both planes (Table 2) show that, for a given area (forearm or thigh), there is no difference in the distribution of the skin fibers densities for the skin at rest between the two age groups. However, it is significant between the two body areas in all directions except for the [40° – 60°] and [140° – 160°] directions for the young group, and [40° – 60°] and [120° – 160°] for the middle-aged group (p-value > 0.05). From the LC-OCT images of Table 1 (horizontal and vertical plane), the fibers network in the young skin seems to be denser than in older skin, particularly in the thigh. But the results in Table 2 do not show a significant difference between the two age groups. A possible explanation is presented in the discussion section.

Correlation tests

The correlation test is performed for the skin data at rest of all included volunteers (21 young volunteers and 21 middle-aged volunteers) and for the skin data during the folding test of 8 volunteers (5 young volunteers and

Table 1. Skin relief and LC-OCT images of the forearm and the thigh at rest (R) and during skin folding test (F) for a young and a middle-aged volunteer. The arrows show the folding direction.

Body area	State	Young			Middle-aged		
		Skin relief	LC-OCT		Skin relief	LC-OCT	
			Horizontal section	Vertical section		Horizontal section	Vertical section
Forearm	R	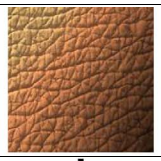	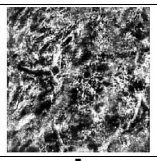	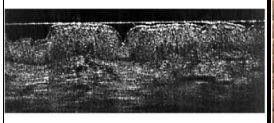	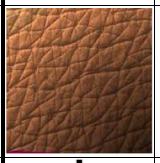	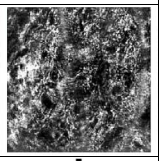	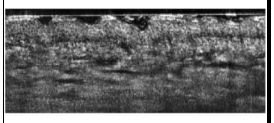
	F			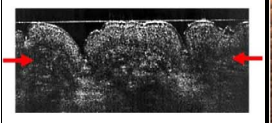	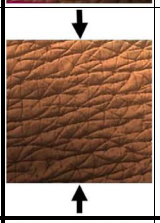	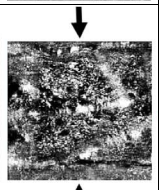	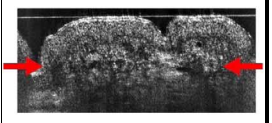
Thigh	R		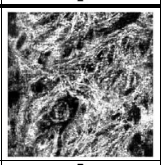	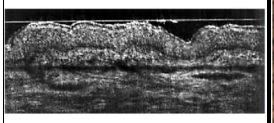	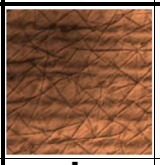	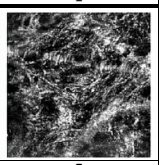	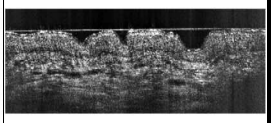
	F	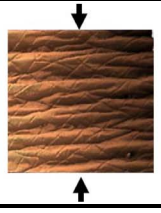	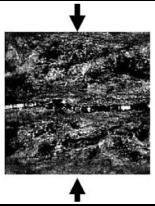	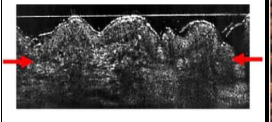	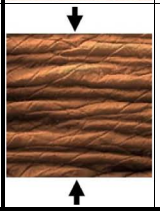	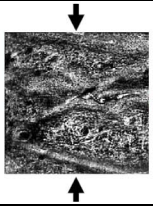	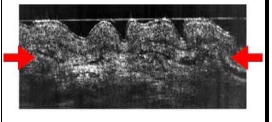

Table 2. Distribution of skin lines and fibers densities according to direction in the horizontal plane (azimuthal) and the vertical plane (polar) for the forearm and the thigh at rest for all volunteers included of the young and the middle-aged groups, and during folding test for 5 young volunteers and 3 middle-aged volunteers. (* for $0.01 < p$-value < 0.05, ** for $0.001 < p$-value < 0.01, *** for p-value < 0.0001).

Area	Forearm		Thigh	
Group	**Young group**	Middle-aged **group**	**Young group**	Middle-aged **group**
Skin relief	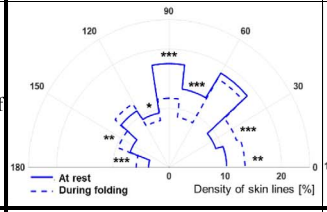	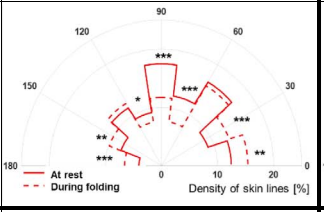	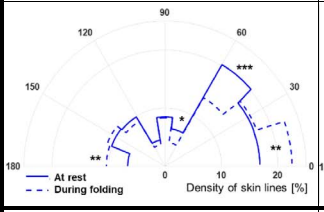	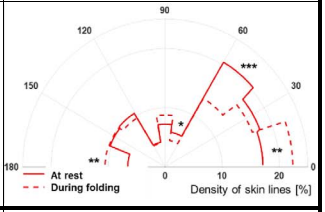
LC-OCT Horizontal plane	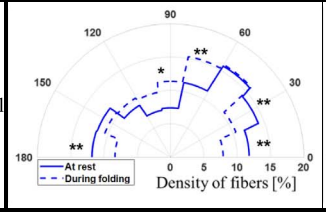	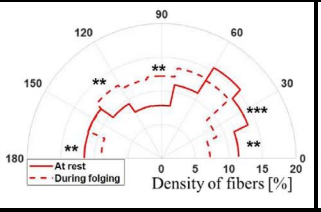	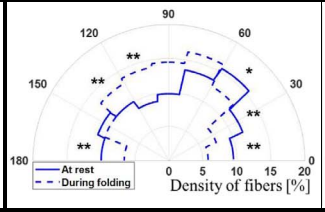	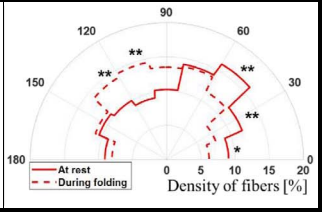
LC-OCT Vertical plane		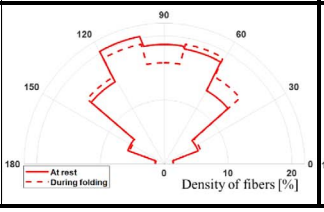	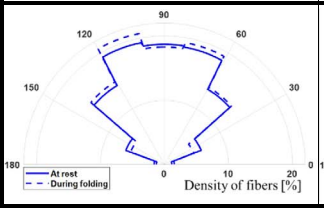	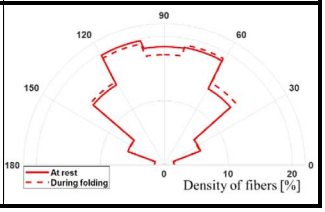

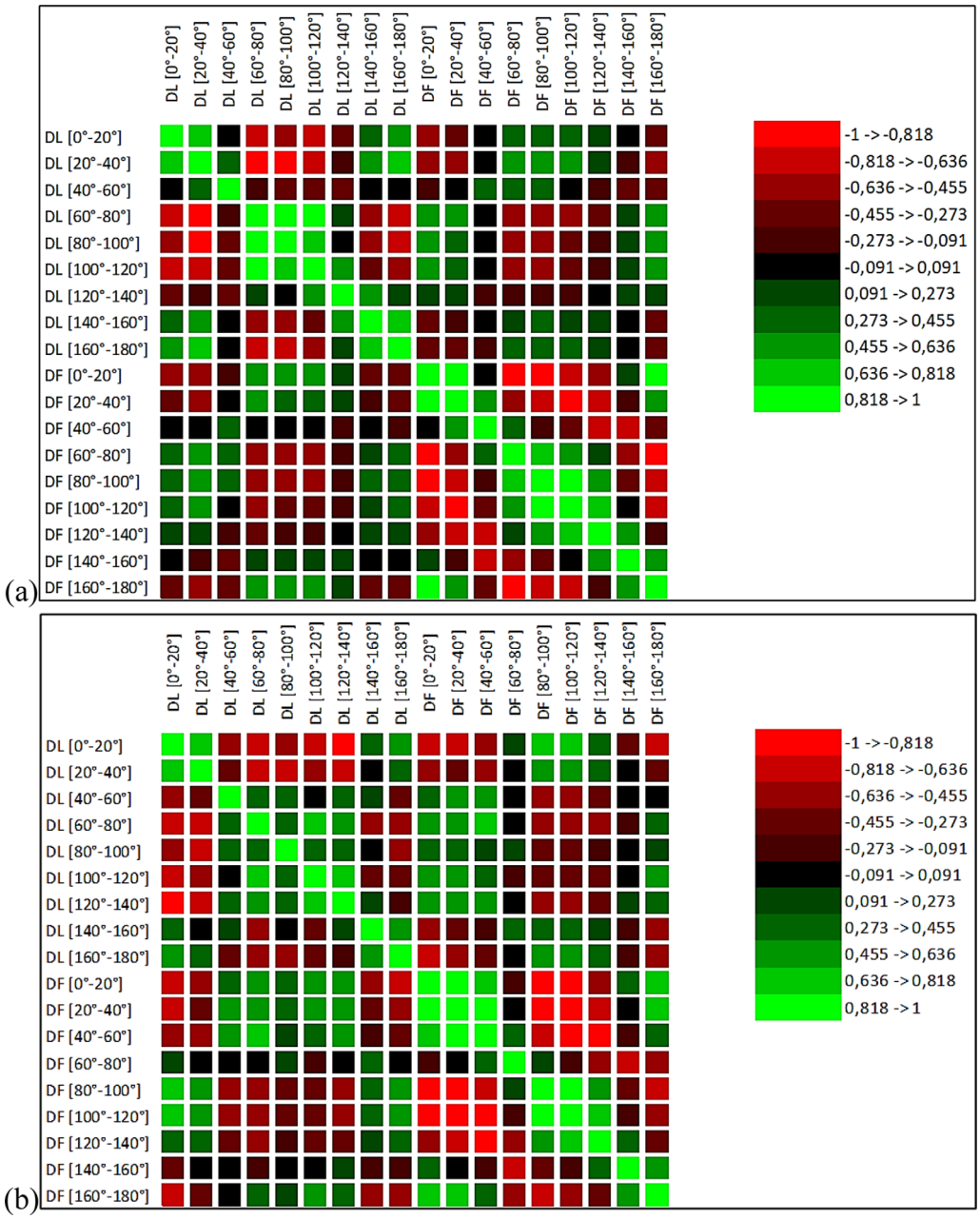

Figure 6. Correlation matrix (a) for the skin at rest (all volunteers included) and (b) for the skin during folding test (for 5 young volunteers and 3 middle-aged volunteers). DL for density of lines, DF for density of fibers.

3 middle-aged volunteers). Figure 6 shows the correlation matrix of the directional analysis of skin relief and skin fibers distribution in the horizontal plane for the forearm and thigh for both age groups at rest (Fig. 6a) and during folding test (Fig. 6b).

For the skin at rest, the correlation coefficient varies between 0.40 and 0.53 for directions between 0° and 90°, and between 0.41 and 0.57 for directions between 90° and 180°. For the skin during the folding test, the correlation coefficient ranges from 0.44 to 0.73 for directions between 0° and 90°, and from 0.40 to 0.70 for directions between 90° and 180°. The relationship between the data of skin surface and the data of skin dermis is good especially when the skin is folded. These correlations show a link between the density of the skin lines and the density of skin fibers depending on the direction. Thus, it can be deduced from this that the skin relief reflects the organization of the fiber network of the dermis.

Discussion and conclusion

The skin was studied in vivo by combining two techniques: one to get information about the skin relief, the second to describe the skin morphology using non-invasive LC-OCT imaging. These analyses, carried out with the skin

at rest and during the folding test, made it possible to identify the directions of maximum density of the lines printed on the surface of the skin and of maximum density of the fibers on the dermis for each zone of the body: the forearm and the thigh.

The comparison of the results obtained by the various experimental tests gives information on the skin surface condition and its condition in volume by analyzing the structure of the skin layers.

For the skin of the forearm at rest, the directions of maximum density of skin lines are [40° – 60°] and [80° – 100°] and the directions of maximum density of the fibers are [40° – 60°]. When the skin folds (Table 2), a reorientation of both the skin lines and fibers occurs and the density of the lines and fibers remains maximum in the preferred directions. The density of the skin lines increases in [0° – 40°] and [140° – 180°] directions and the density of fibers increases in [40° – 140°] directions but both remain maximum in the preferred [40° – 60°] directions for the skin lines, and [40° – 80°] for the skin fibers. These directions correspond to the main direction of skin tension for the forearm as shown in [5, 20, 21].

For the skin of the thigh at rest, the maximum density directions of the skin lines are [0° – 40°] and the maximum density directions of the fibers are [20° – 80°]. During skin folding test (Table 2), the skin lines and fibers are reoriented. The density of the skin lines increases in [0° – 20°] and [160° – 180°] directions and the density of the skin fibers increases in [60° – 140°] directions. The density of skin lines becomes maximum in [0° – 20°] directions and the density of the skin fibers becomes maximum in [40° – 80°] directions. These directions correspond to the main direction of skin tension for the thigh as shown in [5, 20, 21].

Thus, the LC-OCT images, especially in the horizontal section, show quite similar orientations of the organization of the fiber network in the dermis with the line network printed on the skin surface (Tables 1 and 2). The same main directions of skin tension are obtained by analyzing the skin topography and the fibers network, particularly for the forearm. The results of the correlation test confirm the link between the organization of the fiber network and the lines network with a correlation coefficient that varies between 0.40 and 0.57 for the skin at rest and between 0.40 and 0.73 for the skin during the folding test. The topography of the skin surface well reflects the organization of collagen and elastin fibers and the structure of the underlying layers.

The lines and / or the fibers oriented in the directions surrounding the main directions of the skin tension undergo a strong reorientation during the stressing by skin folding. These lines are called skin suppleness lines. It is the fibers oriented in these directions that help to ensure the balance of the skin's tension forces and its flexibility during use or movement of the body limbs. They have a great capacity and ease of adaptation. These results show that there is a link between the orientation of the skin lines on the surface and the organization of the fibers network in the dermis.

The skin surface reflects the state of its layers. So, the skin relief is mainly due to the organization of the collagen and elastin fibers in the dermis. This is also the case when the skin is subjected to mechanical stress.

The results of this study show also that the skin properties are not the same in the two body areas regarding the main directions of tension and suppleness, and the structure of its layers [14]. The main directions of tension depend strongly on the body area. With age, the tension in the skin loosens. This sagging seems to be more important for the skin suppleness lines both on the skin surface or in its volume, especially for the thigh where a significant decrease in line density was noticed in the directions of these lines. The effect of age is noticeable in terms of the topographical properties of the skin, but it is not as pronounced in its volume in terms of fiber density. This could be related to the fact that the age difference between the two groups in this study ([20–30] and [45–55] years old) is not sufficient to see significant differences in skin volume. Ayadh et al. [22] show that there is an increase in glycation end products that accumulate on dermal fibers with age and consequently cause the degradation of their mechanical properties. This would tend to suggest that skin degradation begins with a loss in quality of its main components (dermal fibers) before the loss in quantity. Thus, the aging effect could be remarkable on the skin surface by analyzing its topography and less pronounced in its volume.

The skin tension is therefore largely due to the tension exerted by the dermal fibers. It depends on their organization and their orientation. These results suggest that a simple test on the skin surface could be used to predict the condition in the skin volume and more particularly the condition of the dermal fiber network.

Conflict of interest

The authors have no conflicts of interest.

References

1. Agache P, Maibach HI (2000), Physiologie de la peau et explorations fonctionnelles cutanées, Editions médicales internationales, Cachan.
2. Zahouani H (1998), Spectral and 3D motifs identification of anisotropic topographical components. Analysis and filtring of anisotropic patterns by morphological rose approach. Int J Mach Tools Manuf 38, 97, 615–623.
3. Guinot C, Latreille J, Mauger E, Ambroisine L, Gardinier S, Zahouani H, Guéhenneux S, Tschachler E (2006), Reference ranges of skin micro-relief according to age in French Caucasian and Japanese women. Ski Res Technol 8, 268–278.
4. Zahouani H, Djaghloul M, Vargiolu R, Mezghani S, Mansori MEL (2014), Contribution of human skin topography to the characterization of dynamic skin tension during senescence: Morpho-mechanical approach. J Phys Conf Ser 483, 1, 012012.
5. Ayadh M, Abellan M-A, Didier C, Bigouret A, Zahouani H (2020), Methods for characterizing the anisotropic behavior of the human skin's relief and its mechanical properties in vivo linked to age effects. Surf Topogr Metrol Prop 8, 1, 14002.

6. Ayadh M (2021), Caractérisation de la tension naturelle de la peau humaine in vivo, Université de Lyon opérée au sein de l'Ecole centrale de Lyon, France.
7. Annaidh AN, Bruyère K, Destrade M, Gilchrist MD, Maurini C, Otténio M, Saccomandi G (2012), Automated estimation of collagen fibre dispersion in the dermis and its contribution to the anisotropic behaviour of skin. Ann Biomed Eng 40, 8, 1666–1678.
8. Binda D, Tissot M, Viennet C, Saas P, Muret P, Humbert P (2014), In vitro study of the impact of mechanical tension on the dermal fibroblast phenotype in the context of skin wound healing. J Biomech 47, 14, 3555–3561.
9. Igarashi T, Nishino K, Nayar SK (2005), The appearance of human skin, Columbia University, New York, NY 10027, USA.
10. Vo-dinh T (2003), Biomedical photonics, CRC Press, Boca Raton London New York Washington, D.C.
11. Tran HV (2007), Caractérisation des propriétés mécaniques de la peau humaine in vivo via l'IRM.
12. Li C, Guan G, Reif R, Huang Z, Wang RK (2012), Determining elastic properties of skin by measuring surface waves from an impulse mechanical stimulus using phase-sensitive optical coherence tomography. J R Soc Interf 9, 70, 831–841.
13. Robic J (2018), Automated characterization of skin aging using in vivo confocal microscopy, Medical Imaging. Université Paris Est. NNT: 2018PESC1069.
14. Ayadh M, Abellan MA, Figueiredo S, Pedrazzani M, Cohen E, Bigouret A, Zahouani H (2022), LC-OCT imaging for studying the variation of morphological properties of human skin in vivo according to age and body area: The forearm and the thigh. Dermis 2, 1, 1–12.
15. Guillermin A (2018), Compréhension des phénomènes physiques liés à un plissement de peau : Mesure & caractérisation, École Nationale d'Ingénieurs de Saint – Etienne, Ecole Centrale de Lyon.
16. Kanlayavattanakul M, Lourith N (2015), An update on cutaneous aging treatment using herbs. J Cosmet Laser Ther 17, 343–352.
17. Ogien J, Levecq O, Azimani H, Dubois A (2020), Dual-mode line-field confocal optical coherence tomography for ultra-high-resolution vertical and horizontal section imaging of human skin in vivo. Biomed Opt Express 11, 3, 1327–1335.
18. Ogien J, Daures A, Cazalas M, Perrot J, Dubois A (2020), Line- fi eld confocal optical coherence tomography for three-dimensional skin imaging. Front Optoelectron 13, 4, 381–392.
19. Dubois A, Levecq O, Azimani H, Davis A, Ogien J, Siret D, Barut A (2018), Line-field confocal time-domain optical coherence tomography with dynamic focusing. Opt Express 26, 26, 33534–33542.
20. Langer K (1978), On the anatomy and physiology of the skin I. The cleavability of the cutis. Br J Plast Surg 31, 4, 277–278.
21. Ayadh M, Guillermin A, Abellan M, Bigouret A, Zahouani H (2023), Journal of the Mechanical Behavior of Biomedical Materials The assessment of natural human skin tension orientation and its variation according to age for two body areas: Forearm and thigh. J Mech Behav Biomed Mater 141, August 2022, 105798.
22. Ayadh M, Abellan M, Guillermin A, Bigouret A, Zahouani H (2022), Influence of the biochemical properties of the human skin fibers on its mechanical properties in vivo according to age for two body areas: The forearm and the thigh. Clin Exp Dermatol Ther 7, 4, 1–9.

Cite this article as: Ayadh M, Guillermin A, Abellan M-A, Figueiredo S, Pedrazzani M, et al. 2023. Investigation of the link between the human skin relief and the dermal fibers network by coupling topographic analysis and LC-OCT imaging before and during folding tests. 4open, **6**, 6.